



# HOKKAIDO UNIVERSITY

Title	Formation of hydrotalcite in aqueous solutions and intercalation of ATP by anion exchange
Author(s)	Tamura, Hiroki; Chiba, Jun; Ito, Masahiro et al.
Citation	Journal of Colloid and Interface Science, 300(2), 648-654 <a href="https://doi.org/10.1016/j.jcis.2006.04.007">https://doi.org/10.1016/j.jcis.2006.04.007</a>
Issue Date	2006-08-15
Doc URL	<a href="https://hdl.handle.net/2115/14585">https://hdl.handle.net/2115/14585</a>
Type	journal article
File Information	JCIS.pdf



Formation of Hydrotalcite in Aqueous Solutions and  
Intercalation of ATP by Anion Exchange

Hiroki Tamura\*, Jun Chiba, Masahiro Ito, Takashi Takeda, and Shinichi Kikkawa

Division of Materials Chemistry, Graduate School of Engineering, Hokkaido University,  
Sapporo, 060-8628 Japan

Yasuteru Mawatari and Masayoshi Tabata

Division of Biotechnology and Macromolecular Chemistry, Graduate School of  
Engineering, Hokkaido University, Sapporo, 060-8628 Japan

\*Corresponding author.

Tel.: +81-11-706-6741; Fax: +81-11-706-6740.

E-mail address: h-tamura@eng.hokudai.ac.jp (Hiroki Tamura)

## Abstract

The formation reaction and the intercalation of adenosine triphosphate (ATP) were studied for hydrotalcite (HT), a layered double hydroxide (LDH) of magnesium and aluminum. Hydrotalcite with nitrate ions in the interlayer (HT-NO<sub>3</sub>) was formed (A) by dropwise addition of a solution of magnesium and aluminum nitrates (pH *ca.* 3) to a sodium hydroxide solution (pH *ca.* 14) until the pH decreased from 14 to 10 and (B) by dropwise addition of the NaOH solution to the solution of magnesium and aluminum nitrates with pH increasing from 3 to 10. The precipitate obtained with method (B) was contaminated with aluminum hydroxide and the crystallinity of the product was low, possibly because aluminum hydroxide precipitates at pH 4 or 5 and remains even after HT-NO<sub>3</sub> forms at pH above 8. With method (A), however, the precipitate was pure HT-NO<sub>3</sub> with increased crystallinity, since the solubility of aluminum hydroxide at pH above and around 10 is high as dissolved aluminate anions are stable in this high pH region, and there was no aluminum hydroxide contamination. The formed HT-NO<sub>3</sub> had a composition of [Mg<sub>0.71</sub>Al<sub>0.29</sub>(OH)<sub>2</sub>](NO<sub>3</sub>)<sub>0.29</sub> • 0.58H<sub>2</sub>O. To intercalate ATP anions into the HT-NO<sub>3</sub>, HT-NO<sub>3</sub> was dispersed in an ATP solution at pH 7. It was found that the interlayer nitrate ions were completely exchanged with ATP anions by ion exchange, and the interlayer distance expanded almost twice with a free space distance of 1.2 nm. The composition of HT-ATP was established as [Mg<sub>0.68</sub>Al<sub>0.32</sub>(OH)<sub>2</sub>](ATP)<sub>0.080</sub> • 0.88H<sub>2</sub>O. The increased distance could be explained with a calculated molecular configuration of the ATP as: An ATP molecule is bound to an interlayer surface with the triphosphate group, the adenosine group bends owing to its bond angles and projects into the interlayer to a height of 1 nm, and the adenosine groups aligned in the interlayer support the interlayer distance.

**Keywords:** Hydrotalcite; ATP; Layered compound; Intercalation; Intercalate; Ion exchange

## 1. Introduction

Hydrotalcite (HT), one of the naturally occurring clay minerals, is a layered double hydroxide (LDH) of magnesium and aluminum ions (Fig. 1) with the general formula given as  $[\text{Mg}_{1-x}\text{Al}_x(\text{OH})_2]A^{n-}_{x/n} \cdot m\text{H}_2\text{O}$  [1-4]. The hydroxide layers have the crystal structure of  $\text{Mg}(\text{OH})_2$  (brucite), and have positive charges owing to the extra positive charge of  $\text{Al}^{3+}$  ions. It is due to the charge that this hydroxide develops only in two dimensions, and the layer positive charges,  $x+$ , equivalent to the amount of  $\text{Al}^{3+}$ , are compensated by negative charges of interlayer anions  $A^{n-}$  with water molecules in the interlayer. The interlayer anions may be exchanged with anions in external solutions, and LDHs can be applied to the removal of anionic toxins for water purification, to the separation and concentration of anionic trace elements for analysis, to the preparation of composite materials like supported anion catalysts, to the recovery of precious anionic compounds, and for other applications [5, 6].

Recently, LDHs have attracted attention because such compounds intercalate bioactive molecules with negative charges into the interlayer to form bio-LDH nanohybrids [7-10]. The bio-nanohybrids are electrically neutral and can be transferred into biocells and organs through cell membranes. It is possible that pharmaceutically effective anionic biomolecules, which otherwise cannot be delivered effectively to parts in the bodies, can be used in therapy with such bio-nanohybrids. After giving the dose of the bio-nanohybrid, the intercalated biomolecules will be released to the body fluid with replacement of other anions as the biomolecules in solution are consumed by body parts targeted for therapy. Then the drug concentration level could be kept stable over a long period of time, and controlled drug delivery would become possible with bio-nanohybrids.

The ion exchange ability and capacity of LDHs greatly depend on the purity and crystallinity of the compounds, and their transportation is facilitated by the modification of LDH particles with respect to size, shape, magnetism, and other properties. The authors have reported that well crystallized pure hydrotalcite with nitrate ions in the interlayer ( $\text{HT-NO}_3$ ) can be prepared as a starting compound to prepare bio-HT nanohybrids and that adenosine triphosphate (ATP) can be intercalated into the  $\text{HT-NO}_3$  to form HT-ATP by exchanging the interlayer nitrate ions elsewhere [11].

In this investigation, the process of the formation of hydrotalcite is discussed and it

is explained that the reaction at the high pH region where dissolved aluminate anions are stable results in pure hydrotalcite without the contamination of aluminum hydroxide. The molecular configuration of ATP is calculated and the increased interlayer distance by the intercalation of the ATP is explained in terms of the arrangement of ATP molecules in the interlayer: An ATP molecule is adsorbed to the interlayer surface with the triphosphate group, the adenosine group projects into the interlayer space owing to the bond angles, and the adenosine groups aligned in the interlayer support the increased interlayer distance.

## 2. Experimental

### 2.1. Synthesis of HT-NO<sub>3</sub>

Method A: A solution of magnesium and aluminum nitrates ( $0.24 \text{ mol dm}^{-3} \text{ Mg}^{2+}$  -  $0.12 \text{ mol dm}^{-3} \text{ Al}^{3+}$ , pH *ca.* 3) was added dropwise to a  $1 \text{ mol dm}^{-3}$  NaOH solution (pH *ca.* 14) with stirring in a nitrogen atmosphere at  $60^\circ\text{C}$ . The solution pH decreased and at pH values of 12, 11, and 10, portions of the solution containing white precipitate formed were sampled. The white precipitate was separated by centrifugation, washed with water, and dried in vacuum at  $60^\circ\text{C}$ . For the sample obtained at pH 10, the effect of aging (24 h) was also examined.

Method B: The NaOH solution was added dropwise to the solution of magnesium and aluminum nitrates with pH increasing from 3 to 10 in the order reverse to that of method A. At pH values of 6.5, 8.0, and 10, the precipitate was sampled and separated, washed, and dried with the same procedure as above.

### 2.2. Intercalation of ATP

To intercalate ATP into hydrotalcite, 0.1~1.5 g of HT-NO<sub>3</sub> was put in  $50 \text{ cm}^3$  of a  $0.036 \text{ mol dm}^{-3}$  ATPNa<sub>2</sub> (C<sub>10</sub>H<sub>14</sub>N<sub>5</sub>O<sub>13</sub>P<sub>3</sub>Na<sub>2</sub>) solution with pH adjusted to 7.0 at  $20\sim 60^\circ\text{C}$  (ion exchange method). The reaction time was 10 min to 48 h. Alternatively, a solution of magnesium, aluminum, and ATP ions ( $0.24 \text{ mol dm}^{-3} \text{ Mg}^{2+}$  -  $0.12 \text{ mol dm}^{-3} \text{ Al}^{3+}$  -  $0.12 \text{ mol dm}^{-3}$  ATP) was added dropwise to a  $1 \text{ mol dm}^{-3}$  NaOH solution at  $60^\circ\text{C}$  to reach pH 10 (coprecipitation method). The reaction time was 48 h, and the products

were treated with the same procedure as above.

### 2.3. Characterization

The powder X-ray diffraction analysis of the products was made with a Phillips X'pert-MPD with monochromatized Cu-K $\alpha$  radiation ( $\lambda=0.15418$  nm). The amounts of magnesium and aluminum ions in HT were determined by ICP analysis after the sample was dissolved with sulfuric acid. The sample solutions were analyzed for phosphorus by the molybdenum blue method (visible absorption spectrophotometry), and the amount of phosphorus was converted to ATP as one molecule of ATP contains one triphosphate group. Nitrate ions were determined by UV-spectrophotometry, interlayer water by TG-DTA, and carbon, hydrogen, and nitrogen (CHN) in HT-ATP by the elemental analysis.

## 3. Results and discussion

### 3.1. Formation of HT-NO<sub>3</sub>

Figure 2 shows the XRD patterns for the precipitate obtained by method A. The diffraction peaks could be indexed as hydrotalcite and are represented by the lattice parameters (hexagonal):  $a = 0.305$  nm and  $c = 0.887$  nm. It is shown that the precipitate obtained at pH 12 exhibits the diffraction peaks characteristic of hydrotalcite. This indicates that the pH range where hydrotalcite forms extends to the very high pH region. With decreasing pH the diffraction peaks become less sharp, but the peaks of the pH 10 precipitate become very sharp after aging for 24 h.

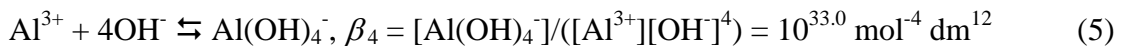
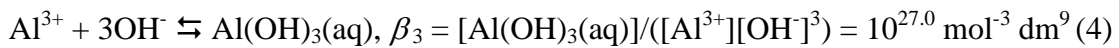
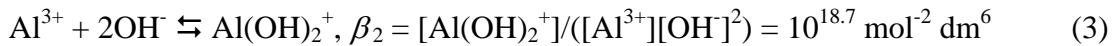
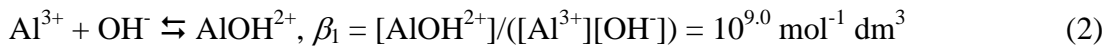
Table 1 shows the Mg<sup>2+</sup>/Al<sup>3+</sup> ratio of the precipitate and the layer positive charge  $x+$  vs. pH. At pH 12, the Mg<sup>2+</sup>/Al<sup>3+</sup> ratio is larger than the initial ratio of 2.0 for the solution, and it decreases with decreasing pH; the layer positive charge  $x+$  increases with decreasing pH as the amount of Al<sup>3+</sup> incorporated increases. The results for HT-NO<sub>3</sub> obtained at pH 10 after 24 h aging are different from the previous results [11]. The amounts of interlayer nitrate ions and interlayer water molecules of this aged product are shown in Table 2, and these results combined with the Mg<sup>2+</sup>/Al<sup>3+</sup> ratio of 2.40 (Table 1) gives the composition: [Mg<sub>0.71</sub>Al<sub>0.29</sub>(OH)<sub>2</sub>](NO<sub>3</sub>)<sub>0.29</sub> • 0.58H<sub>2</sub>O.

The XRD results for the products obtained with method B are shown in Fig. 3. The product formed at pH 6.5 has poor crystallinity and contains aluminum hydroxide, but the product formed at pH 8.0 shows the diffraction peaks characteristic of hydrotalcite. Bocclair et al. [2] reported that when titrating magnesium and aluminum nitrates solution with sodium hydroxide solution, the titration curve shows a plateau around pH 8 where hydrotalcite forms by conversion of the aluminum hydroxide that has formed at lower pH. However, Fig. 3 shows that the product at pH 8.0 is contaminated with aluminum hydroxide, and the conversion is not complete. A higher pH would facilitate the conversion as the pH 10 products show better crystallinity.

From this it is concluded that method A with a pH of 10 and an aging time of 24 h provides better crystallized pure hydrotalcite with a larger ion exchange capacity than method B.

### 3.2. Stability of $Al(OH)_3$ , $Mg(OH)_2$ , and $HT-NO_3$

The stabilities of aluminum and magnesium hydroxides are shown in Fig. 4. The relevant reactions and equilibrium constants were taken from [12] and transformed to forms appropriate for this study: For aluminum hydroxide,

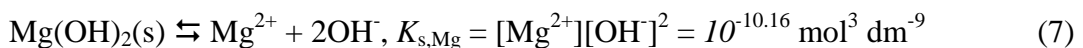


where  $K_{s,Al}$  is the solubility product of aluminum hydroxide,  $\beta_1$  through  $\beta_4$  are the stability constants of aluminum hydroxo complexes, all these are concentration constants. Then the solubility of aluminum hydroxide  $S_{Al}$  is given as:

$$S_{Al} = K_{s,Al}(1 + \beta_1[OH^-] + \beta_2[OH^-]^2 + \beta_3[OH^-]^3 + \beta_4[OH^-]^4)/[OH^-]^3 \quad (6)$$

The solubility  $S_{Al}$  was calculated as a function of pH with the ionic product of water  $K_w$  ( $10^{-14} \text{ mol}^2 \text{ dm}^{-6}$ ) as shown in Fig. 4. It has a minimum at pH around 6, and aluminum hydroxide dissolves in both acid (pH < 4) and alkali (pH > 11) solutions.

The solubility of magnesium hydroxide was calculated similarly according to the following equations:



$$S_{\text{Mg}} = K_{\text{s,Mg}}/[\text{OH}^-]^2 \quad (8)$$

where  $K_{\text{s,Mg}}$  is the solubility product and  $S_{\text{Mg}}$  is the solubility of magnesium hydroxide. Figure 4 shows that the log of  $S_{\text{Mg}}$  decreases linearly with increasing pH.

The maximum values of  $S_{\text{Mg}}$  and  $S_{\text{Al}}$  here are 0.24 and 0.12 mol dm<sup>-3</sup>, equal to the concentrations of these ions in the magnesium and aluminum nitrates solution used to prepare hydrotalcite. With method B, pH increases from *ca.* 3 of the solution to higher values, and aluminum hydroxide starts to form even at pH 4.0, and can remain and contaminate the hydrotalcite that forms at higher pH (above 8). With method A, the initial pH is *ca.* 14 of the NaOH solution used to prepare hydrotalcite, and when the magnesium and aluminum nitrates solution is introduced into the pH 14 solution, aluminum ions become aluminate anions  $\text{Al}(\text{OH})_4^-$  that dissolve in the solution. As a result, no aluminum hydroxide precipitates and there is no contamination of the hydrotalcite with aluminum hydroxide. The very stable dissolved state of  $\text{Al}(\text{OH})_4^-$  may explain why the  $\text{Mg}^{2+}/\text{Al}^{3+}$  ratio of the hydrotalcite at the high pH was larger than the 2.0 of the solution composition (Table 1).

The diagram shows that magnesium hydroxide can precipitate at high pH, but the hydrotalcite obtained at high pH was not contaminated with magnesium hydroxide as the XRD indicates (Fig. 2). This suggests that hydrotalcite is preferentially formed by the reaction between  $\text{Mg}^{2+}$  and  $\text{Al}(\text{OH})_4^-$  and the deposition of magnesium hydroxide does not take place even in the very high pH region. For the low pH limit of the formation of hydrotalcite with high purity and high crystallinity, a pH of 9 was chosen according to the discussion above with method B. The pH range for the hydrotalcite formation that overlaps the stability regions of aluminum and magnesium hydroxides is indicated in Fig. 4 (HT-NO<sub>3</sub> shaded area).

### 3.3. Intercalation of ATP

The intercalation of ATP into hydrotalcite by ion exchange was attempted by introducing the HT-NO<sub>3</sub> into the ATP solution with a pH of 7. The ATP molecule is composed of an adenosine group and a triphosphate group with four acid hydroxyl groups. Three of the acid groups are relatively strong acids with p*K* values around 1 and 2 and the p*K* of the final hydroxyl group is 7 [13]. Thus at pH 2-7, ATP has a charge of 3-, and at pH above 7 the final hydroxyl group dissociates to result in the charge of ATP

of 4-. Diffraction pattern (a) in Fig. 5 shows the peaks for HT-ATP obtained by the ion exchange method at pH 7 and 60°C with a reaction time of 48 h. Compared with Fig. 2, before intercalation, the (001) and (002) diffraction lines shift to much lower  $2\theta$  angles while the shift of the (110) line is small. The lattice parameters (hexagonal) are:  $a = 0.304$  nm and  $c = 1.703$  nm, showing that the interlayer distance ( $c$ ) increased almost twice from 0.887 nm to 1.703 nm possibly due to intercalated ATP molecules. The elemental analysis showed no nitrate ions left in the interlayer and the amounts of magnesium, aluminum, ATP, and interlayer water are shown in Table 3. The measured Mg/Al ratio and the assumption of the OH<sup>-</sup> content as twice the content of all the layer metal ions like in the brucite Mg(OH)<sub>2</sub> structure result in a layer positive charge of 0.32+. The interlayer negative charge 0.32- leads to a charge of the respective ATP of 4.3- for the measured ATP content (Table 3) corresponding to (ATP)<sub>0.074</sub>. However, the largest possible ATP charge is 4-. From the ATP charge 4-, the ATP content was deduced as (ATP)<sub>0.080</sub> to satisfy the electric neutrality of the intercalate. The deduced ATP content is close to the measured result, and with the deduced ATP content the composition of HT-ATP was established as [Mg<sub>0.68</sub>Al<sub>0.32</sub>(OH)<sub>2</sub>](ATP)<sub>0.080</sub> • 0.88H<sub>2</sub>O.

For the ion exchange experiment, HT-NO<sub>3</sub> was dispersed in an ATP solution with pH 7 at 60°C with agitation. Some HT-NO<sub>3</sub> dissolves by this dispersion, and as a result the solution pH increased to a value higher than the initial value. The final acid hydroxyl group of ATP with pK 7 would have dissociated in the solution leading to a charge of 4-. However, Choy et al. [10] obtained an intercalate containing ATP with the charge 3-, and the pH values do not seem exactly the same in the two investigations.

There is a slight enrichment of Al in HT-ATP compared with HT-NO<sub>3</sub>, and this can be attributed to a preferential dissolution of Mg from HT-NO<sub>3</sub> during the ion exchange experiment. From the HT-NO<sub>3</sub>, magnesium hydroxide would dissolve more easily than aluminum hydroxide owing to its larger solubility around pH 7, resulting in a hydrotalcite with a higher Al content.

Also, the amount of interlayer water of HT-ATP is larger than that of HT-NO<sub>3</sub>, indicating an increase in the hydrophilicity of the interlayer by the ATP incorporation.

Choy et al. [8, 10] reported the interlayer distance of HT-ATP 1.94 nm larger than the 1.703 nm obtained here. The different interlayer distances can be due to different compositions of the two intercalates. The ATP intercalate obtained by Choy et al. contains carbonate ions and 1.0H<sub>2</sub>O [10], while the intercalate here contains 0.88H<sub>2</sub>O

without carbonate. The higher extent of hydration and the inclusion of carbonate ions may have resulted in the larger interlayer distance. The different compositions may be due to differences in the experimental conditions of the two investigations, especially in the shielding of the solution from air and in the drying of the product after washing. For the HT-NO<sub>3</sub> before ATP intercalation, there is a much larger difference in the water content, 1.22H<sub>2</sub>O by Choy et al. and 0.58H<sub>2</sub>O here.

#### *3.4. ATP molecules in the Interlayer*

The molecular configuration of ATP was analyzed by the MMFF94 force field program (Spartan '04 Windows, version 1.03, Wavefunction, Inc. [14]) to evaluate how the large ATP molecules are situated in the narrow interlayer space and how the layer structure is sustained. For the analysis, the usual bond lengths and bond angles were applied to the bonds within ATP and the rotation of atoms around the bond axis was left free to attain the lowest energy of the molecule, and the results are shown in Fig. 6. The triphosphate group is at the bottom, and the adenosine group (adenine and ribose) stretches up to a height of 1 nm and a width of 1 nm.

The top view of the layer of hydrotalcite is shown as edge-sharing metal hydroxide octahedrons in Fig. 7(a). The Mg<sup>2+</sup>/Al<sup>3+</sup> ratio here is assumed to be 2 to represent the hydrotalcite obtained in this investigation. Among the metal ions designated with circles in the center of octahedrons, the Al<sup>3+</sup> ions bringing about a net charge of 1+ are indicated by plus signs in the Figure. The four neighboring positive charge sites as indicated by the diamond may be regarded as a unit of layer positive charges that are distributed uniformly in the layer. In Fig. 7(b), a triphosphate group is shown as three corner-sharing tetrahedrons of phosphorous oxide, and oxide ion sites with a charge of 1- due to the proton dissociation of hydroxyl groups are indicated by minus signs here. If this triphosphate group with a charge of 4- is superposed on the diamond with a charge of 4+, three of the four sites on the triphosphate group fit very closely to three of the four neighboring sites on the interlayer surface, but the remaining site has a poorer fit. However, the deviation here is small, and the positive and the negative charge units would overlap with position adjustments to maximize the electrostatic attraction. It can be assumed that the ATP molecule is adsorbed to the layer surface by the attraction between the triphosphate negative charge and the layer positive charge.

A model of the arrangement of the ATP molecules adsorbed on the two opposing surfaces in an interlayer is shown in Fig. 8. One hydroxide layer, that is linked octahedrons of hydroxide ions each with a radius of 0.15 nm, has a thickness of 0.5 nm. Then the thickness of the interlayer free space (gallery height) of HT-ATP, the difference between the interlayer distance of 1.7 nm and the layer thickness of 0.5 nm, is 1.2 nm. The gallery height of HT-NO<sub>3</sub> before ATP intercalation can be evaluated similarly as 0.387 nm. The adenosine group of an ATP molecule bound to the layer surface would project into the interlayer space to a height of 1 nm as calculated for a free ATP molecule above. The adenosine groups stretching upwards are aligned in the interlayer space and the increase in interlayer free distance to 1.2 nm can be explained with the molecular height of the ATP of 1 nm. It may be assumed that an ATP molecule occupies a volume of a cylinder with a height of 1 nm and a width of 1 nm as shown in Fig. 6. Then the projected area of an ATP molecule can be regarded as the same as the cross-sectional area of the cylinder of 0.79 nm<sup>2</sup>. Crystallographically, the diamond of four neighboring positive charges is constituted of twelve octahedrons as indicated by the shaded area in Fig. 7(a), and the projected area of these twelve octahedrons can be calculated to be 0.94 nm<sup>2</sup>, larger than the projected ATP area. Further, the layer positive charges are counterbalanced by adsorbing anions on both sides of a layer (the over and under sides of the layer), and for one of the two surfaces of a layer, only half of the charges adsorb anions. Therefore, there is no steric hindrance in the arrangement with the ATP molecules fully loaded in the interlayer.

The model calculations of the ATP configuration were made for a free ATP molecule in vacuum. The interlayer distance of hydrotalcite intercalated with ATP and the maximum loading of ATP in the interlayer can be explained well with the height and the cross-sectional area of free ATP molecules.

A triphosphate group of an ATP molecule cannot be in contact with the two opposing layers because the thickness of the triphosphate group of 0.54 nm, equivalent to the height of a tetrahedron of oxide ions each with a radius of 0.145 nm, is much smaller than the gallery height of 1.2 nm. Then the triphosphate groups cannot bind the layers and the layer structure would be sustained by the attractive interactions between aligned adenosine groups of ATP. With this model, the increased number of water molecules in the interlayer after the intercalation of ATP can be ascribed to hydration of the strongly hydrophilic triphosphate groups.

### 3.5. Rate of Intercalation

The intercalation rate and the effect of temperature on intercalation were examined. The incorporation of ATP was completed within several tens of minutes and the intercalation rate is rapid. However, it was found that 48 h were necessary to obtain well-defined HT-ATP, indicating that it takes time for the intercalates to be ordered. Within the temperature range 20~60°C, the product obtained at 60°C attained the best crystallinity.

### 3.6. Coprecipitation of ATP

Diffraction pattern (b) in Fig. 5 shows the peaks for the product obtained by intercalation of ATP by the coprecipitation method. The (110) peak is clearly observed at the same position as that of HT-ATP, but the 001 and (002) peaks are not clear. When this sample was made in contact with a solution containing carbonate ions, it became HT-CO<sub>3</sub>, showing clear (001) and (002) peaks (Fig. 5). The coprecipitation product with ATP is likely to have a layer structure, and the unclear XRD patterns may be due to random arrangements of the ATP molecules in the interlayer. The chemical composition of the coprecipitation product  $[\text{Mg}_{0.68}\text{Al}_{0.32}(\text{OH})_2](\text{ATP})_{0.084}\cdot 0.82\text{H}_2\text{O}$  clearly indicates the incorporation of ATP in the structure. Long aging with higher temperatures would increase the ordering of the ATP molecules in the structure.

## 4. Summary

This study showed that hydrotalcite with little contamination of aluminum hydroxide precipitates when adding magnesium and aluminum nitrates solution to sodium hydroxide solution. Further, large ATP molecules intercalate into hydrotalcite by exchanging small interlayer nitrate ions. As a result, the interlayer free distance (gallery height) increased to 1.2 nm from 0.387 nm. The molecular configuration of ATP was established by model calculations and it was suggested that: An ATP molecule is adsorbed by a positively charged layer surface with a negatively charged triphosphate group. The adenosine group of the ATP molecule stretches up into the

interlayer space to a height of 1 nm supporting the interlayer free space. The adenosine groups of the ATP adsorbed on two opposing layer surfaces bind the two hydroxalcite layers by attractive interactions.

### **Acknowledgment**

This work was supported by a grant-in-aid for Scientific Research (14580580) and also by a special Joint-Undertaking grant of Hokkaido University and Hokkaido Government from the Ministry of Education, Culture, Sports, Science and Technology, Japan.

## References

- [1] S. Miyata, *Clays and Clay Minerals* 23 (1975) 369.
- [2] J. W. Boclair, P. S. Braterman, *Chem. Mater.* 11 (1999) 298.
- [3] J-M. Oh, S-H. Hwang, J-H. Choy, *Solid State Ionics* 151 (2002) 285.
- [4] N. Iyi, T. Matsumoto, Y. Kaneko, K. Kitamura, *Chem. Mater.* 16 (2004) 2926.
- [5] L. Lei, F. Millange, R. I. Walton, D. O'Hara, *J. Mater. Chem.* 10 (2000) 1881.
- [6] L. Li, S. Luo, X. Duan, *J. Mater. Sci. Lett.* 21 (2002) 439.
- [7] J-H. Choy, S-Y. Kwak, J-S. Park, Y-J. Jeong, J. Portier, *J. Am. Chem. Soc.* 121 (1999) 1399.
- [8] J-H. Choy, S-Y. Kwak, Y-J. Jeong, J-S. Park, *Angew. Chem. Int. Ed.* 39 (2000) 4042.
- [9] S. Aisawa, S. Takahashi, W. Ogasawara, Y. Umetsu, E. Narita, *J. Solid State Chem.* 162 (2001) 52.
- [10] J-H. Choy, S-Y. Kwak, J-S. Park, Y-J. Jeong, *J. Mater. Chem.* 11 (2001) 1671.
- [11] H. Tamura, J. Chiba, M. Ito, T. Takeda, S. Kikkawa, *Solid State Ionics* 172 (2004) 607.
- [12] J.J. Morgan, W. Stumm, *Aquatic Chemistry*, third ed., Wiley, New York, 1996, p. 326, 362.
- [13] E.E. Conn, P.K. Stumpf, G. Bruening. R.H. Doi, *Outlines of Biochemistry*, fifth ed., translated by N. Tamiya, T. Yagi, Tokyo Kagakudojin, Tokyo, 1988, p. 288.
- [14] T.A. Halgren, *J. Comput. Chem.* 17 (1996) 490.

## Table legends

Table 1  $Mg^{2+}/Al^{3+}$  ratio and the layer charge,  $x_+$ , of HT- $NO_3$  obtained from solutions with an  $Mg^{2+}/Al^{3+}$  ratio of 2.0

Table 2 Contents of  $NO_3^-$  and  $H_2O$  in HT- $NO_3$  precipitated at pH 10 with 24 h aging and dried in vacuum at  $60^\circ C$  for 3 h

Table 3 Composition of HT-ATP dried in vacuum at  $60^\circ C$  for 3 h

## Figure legends

Fig. 1 Layer structure of hydrotalcite.

Fig. 2 XRD patterns of hydrotalcite with nitrate ions in the interlayer obtained by method A at different pH and aging time.

Fig. 3 XRD patterns of hydrotalcite with nitrate ions in the interlayer obtained by method B at different pH.

Fig. 4 Domain diagram of  $Al(OH)_3$ ,  $Mg(OH)_2$ , and HT- $NO_3$ .

Fig. 5 XRD patterns of hydrotalcite with ATP ions in the interlayer obtained by (a) ion exchange and (b) coprecipitation methods.

Fig. 6 Configuration of an ATP molecule by model calculations.

Fig. 7 Schematic representations of (a) hydrotalcite layer and (b) triphosphate group.

Fig. 8 Model of the arrangement of ATP molecules in the interlayer.

Table 1  $\text{Mg}^{2+}/\text{Al}^{3+}$  ratio and the layer charge,  $x+$ , of HT- $\text{NO}_3$  obtained from solutions with an  $\text{Mg}^{2+}/\text{Al}^{3+}$  ratio of 2.0

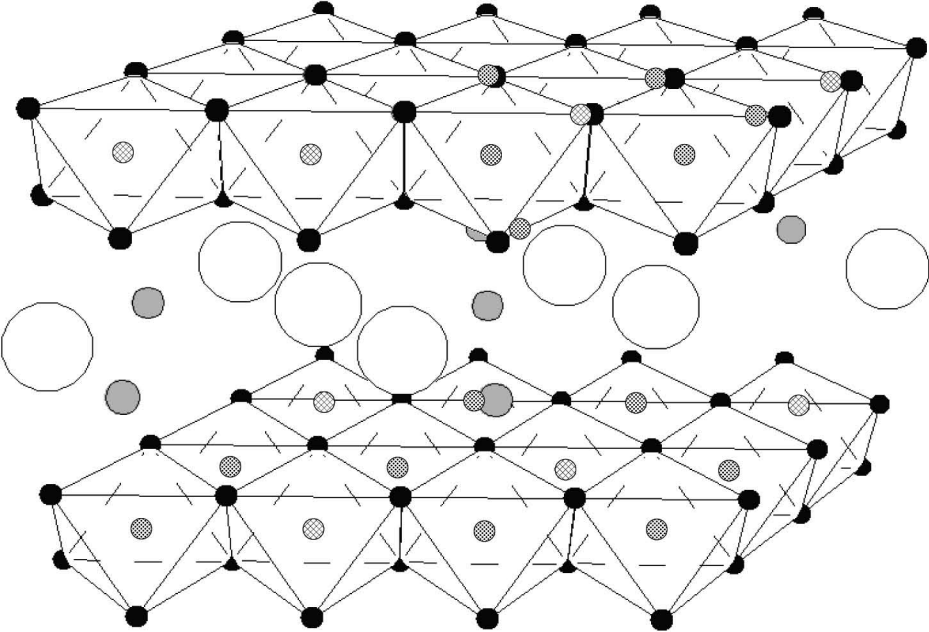
pH	$\text{Mg}^{2+}/\text{Al}^{3+}$	$x+$
12	2.94	0.25+
11	2.60	0.27+
10	2.55	0.28+
10 (24 h)	2.40	0.29+

Table 2 Contents of  $\text{NO}_3^-$  and  $\text{H}_2\text{O}$  in HT- $\text{NO}_3$  precipitated at pH 10 with 24 h aging and dried in vacuum at  $60^\circ\text{C}$  for 3 h

$\text{NO}_3^-/\text{mol g}^{-1}$	$\text{H}_2\text{Owt}\%$
$3.26 \times 10^{-3}$	12.0

Table 3 Composition of HT-ATP dried in vacuum at  $60^\circ\text{C}$  for 3 h

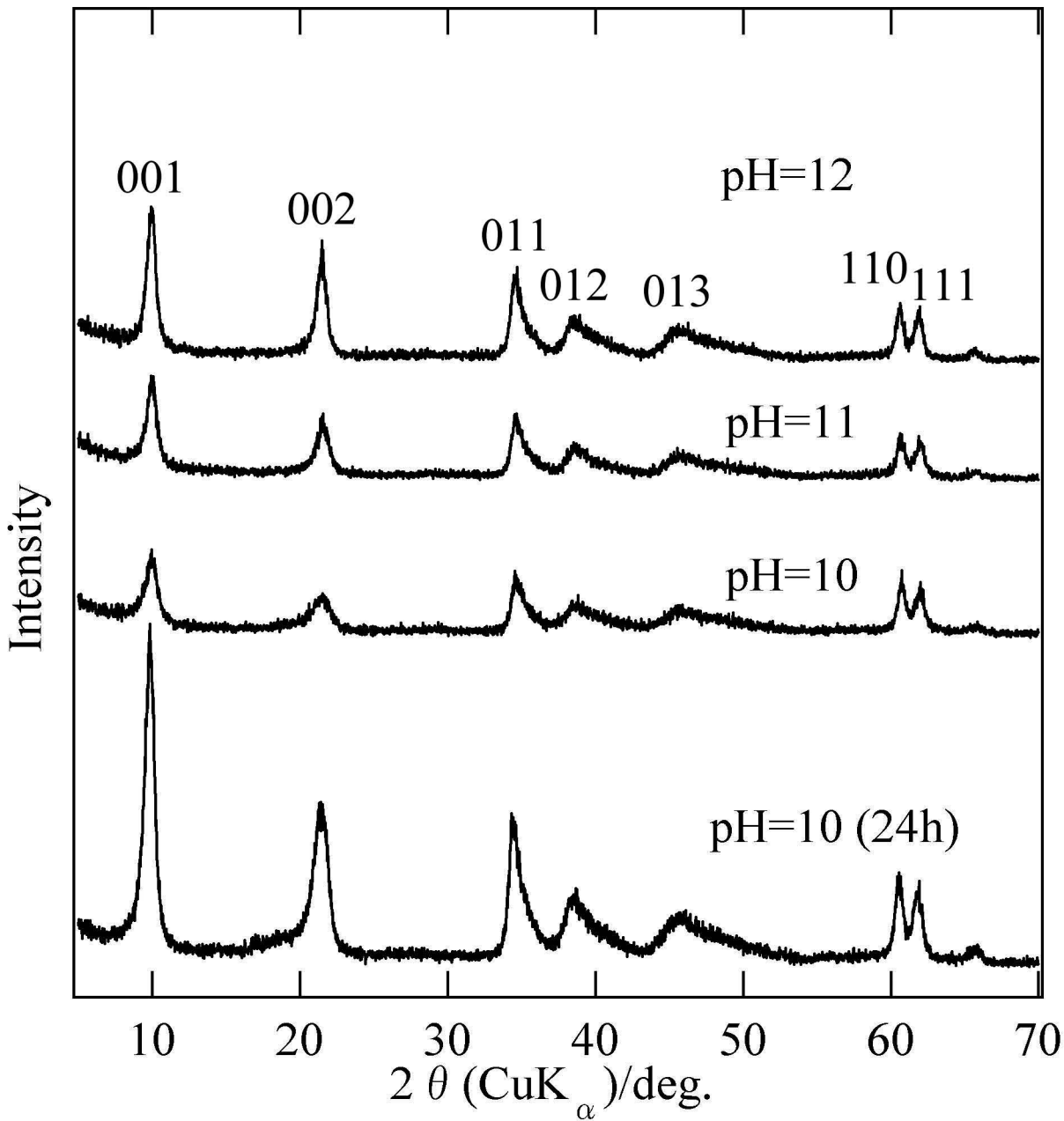
$\text{Mg}^{2+}/\text{mol g}^{-1}$	$\text{Al}^{3+}/\text{mol g}^{-1}$	$\text{ATP}/\text{mol g}^{-1}$	$\text{H}_2\text{Owt}\%$
$5.59 \times 10^{-3}$	$2.64 \times 10^{-3}$	$6.11 \times 10^{-4}$	13.5

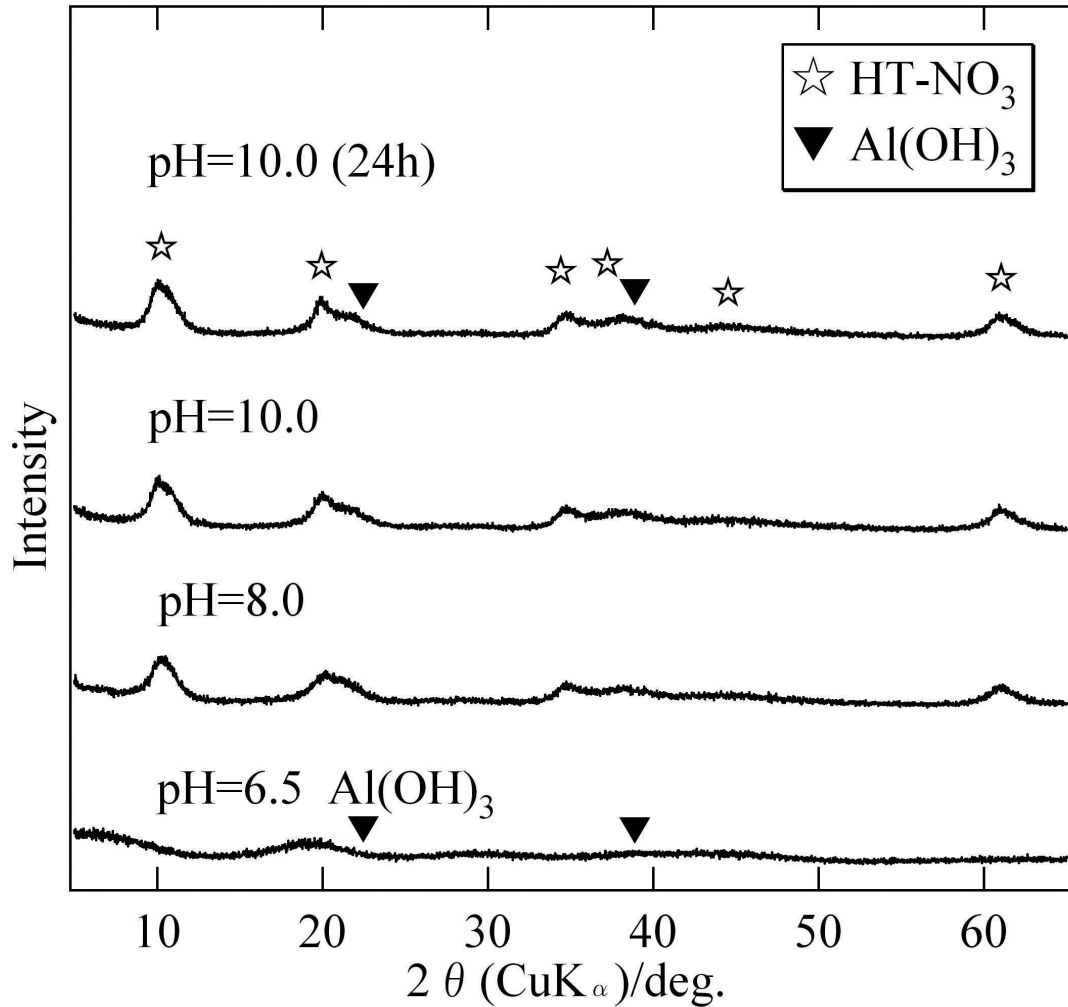


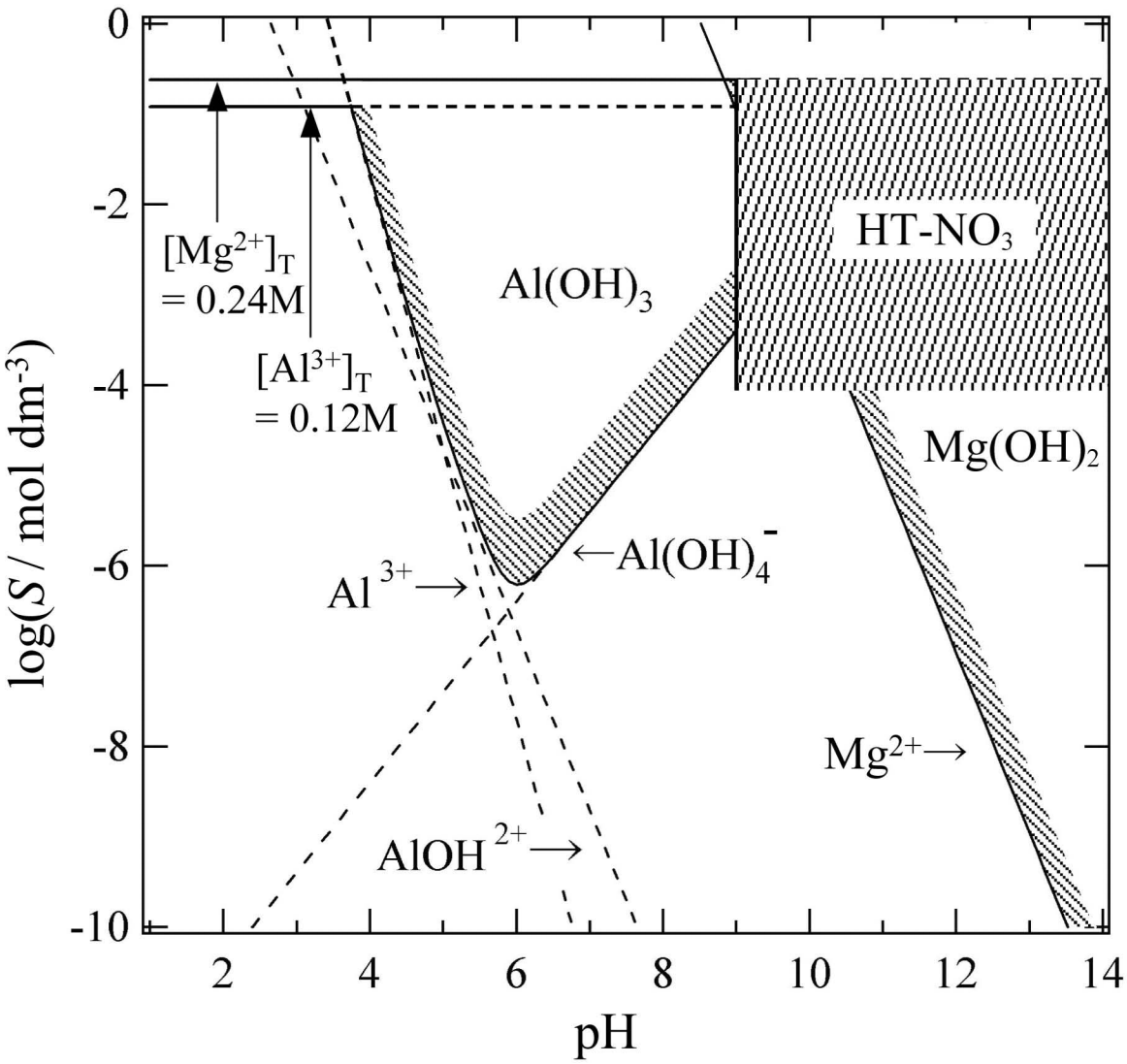
← Host layer:  $\odot$  Mg<sup>2+</sup>,  $\otimes$  Al<sup>3+</sup>,  $\bullet$  OH<sup>-</sup>

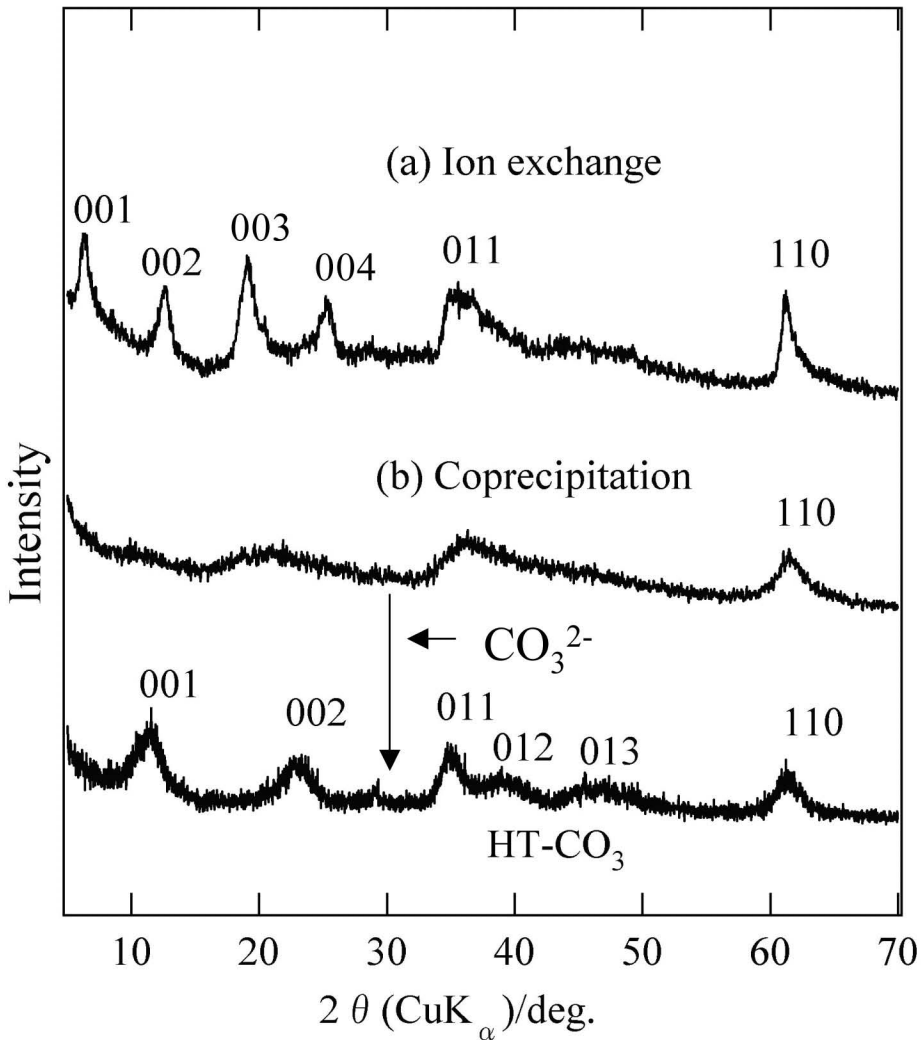
← Guest layer:  $\circ$  A<sup>n-</sup> (anions)

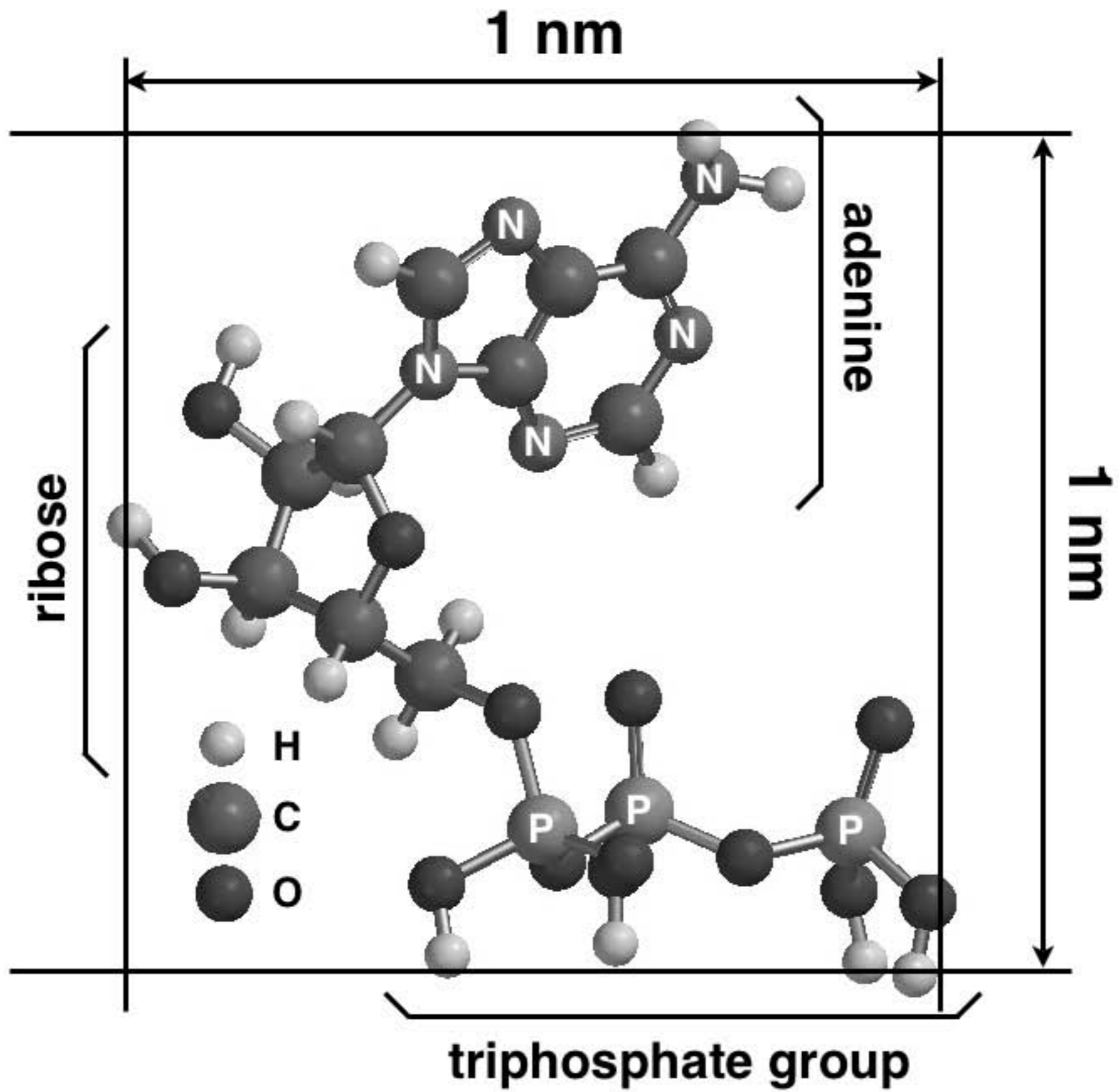
$\ominus$  H<sub>2</sub>O

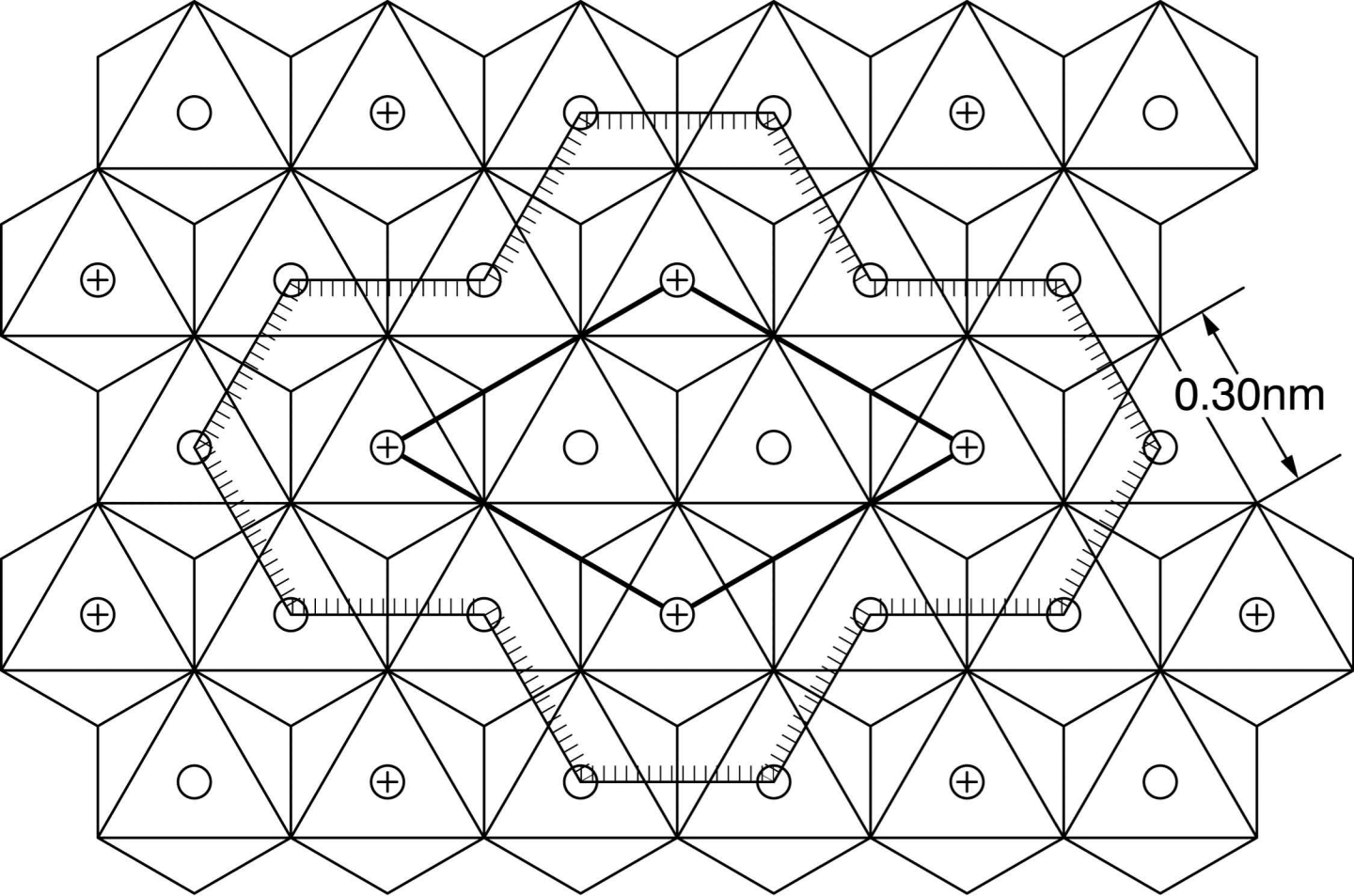




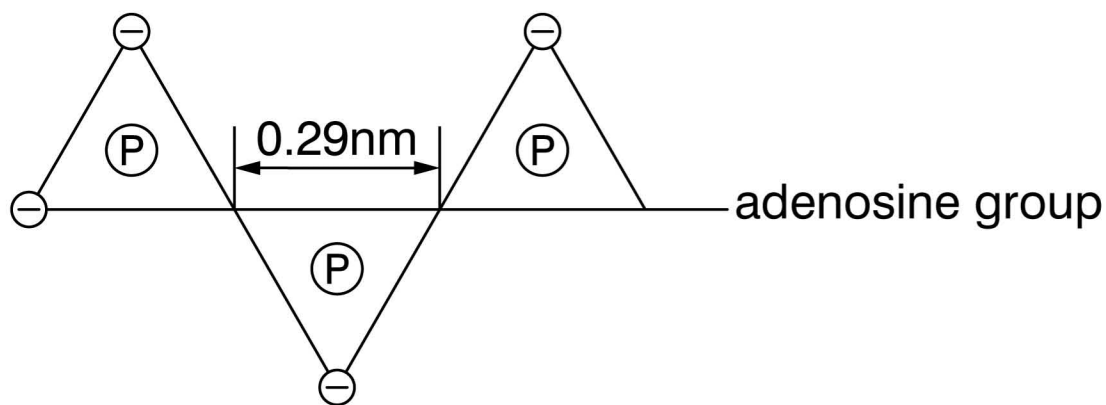








(a) Hydrotalcite layer as linked hydroxide octahedrons



(b) Triphosphate group as linked oxide tetrahedrons

